An Efficient and Compact Compressed Sensing Microsystem for Implantable Neural Recordings

Jie Zhang, *Student Member, IEEE*, Yuanming Suo, *Student Member, IEEE*, Srinjoy Mitra, *Member, IEEE*, Sang (Peter) Chin, Steven Hsiao, Refet Firat Yazicioglu, *Member, IEEE*, Trac D. Tran, *Senior Member, IEEE*, and Ralph Etienne-Cummings, *Fellow, IEEE*

***Abstract*—Multi-Electrode Arrays (MEA) have been widely used in neuroscience experiments. However, the reduction of their wireless transmission power consumption remains a major challenge. To resolve this challenge, an efficient on-chip signal compression method is essential. In this paper, we first introduce a signal-dependent Compressed Sensing (CS) approach that outperforms previous works in terms of compression rate and reconstruction quality. Using a publicly available database, our simulation results show that the proposed system is able to achieve a signal compression rate of 8 to 16 while guaranteeing almost perfect spike classification rate. Finally, we demonstrate power consumption measurements and area estimation of a test structure implemented using TSMC 0.18 μm process. We estimate the proposed system would occupy an area of around 200μm$\times$300 μm per recording channel, and consumes 0.27 μW operating at 20 KHz.**

***Index Terms*—Compressed sensing (CS), dictionary learning, hardware implementation, multi-electrode arrays (MEA).**

I. Introduction

A. The Need for An On-Chip Signal Compression System

ONE of the major challenges in building a low power wireless implantable neural signal recording system is the reduction of the signal transmission power. Neural action potentials (APs), also referred to as spikes, have a bandwidth up to 10 KHz and amplitude ranging from 50 μV to 500 μV [1]. When the Multi-Electrode Array (MEA) containing up to hundreds of electrodes is used to capture the neuronal activities of a certain brain area, the data acquired by the recording system is on the order of megabytes per second. To transmit this large volume of data off-chip wirelessly requires power consumption of tens of mW [1]. To reduce transmission power consumption, researchers have investigated into various compression techniques aiming to reduce the volume of the data at the sensor node before they are transmitted off-chip.

B. Priors Works

Spike Detection and windowing method is widely used for activity based compression. It transmits the signal segments containing spike activity while neglecting the signal segments that do not contain any significant activities [2]–[6]. The most common spike detection is the threshold crossing detection method. Its implementation requires few additional circuit components which occupy a small layout area while consuming very limited power. However, this method preserves the shape of the spike while discarding the inter-spike signal, which contains undetected spikes and other important neural voltage variations. Therefore this compression method cannot be used when researchers are interested in analyzing the entire neural signal.

On the other extreme, there lies the nearly lossless alternative of wavelet transform based compression method [7], [8]. After the signals are transformed into their wavelet representations using an on-chip circuit, only a fraction of the significant wavelet coefficients are transmitted off-chip. Wavelet transform based systems are able to achieve impressive compression rates while maintaining excellent signal reconstruction quality. However, an ASIC implementation of wavelet transform is less efficient in terms of area and power consumption as it requires implementation of digital filters and on-chip memories operating at a speed above signal Nyquist frequency.

Recently, the development in the field of Compressed Sensing (CS) has inspired a family of new compression systems that use simple circuitry and have the potential to achieve compression performance similar to that of the wavelet transform [1], [9]–[11]. The CS compression steps can be implemented using digital accumulators operating at signal Nyquist rate. The random sensing mechanism of the system is also independent from signal representation basis. Thus the users have the flexibility to choose the best signal representation basis for recovery. For example, the user may choose to reconstruct a signal from one channel using wavelets, while reconstructing another channel using Gabor frames without reconfiguring the on-chip hardware. Lastly, the CS based systems are also very flexible as their power consumption, compression rate, and recovery quality can be adjusted to meet the desired tradeoff of the users by simply turning on/off the mixing accumulators.

Manuscript received May 03, 2013; revised July 23, 2013; accepted September 02, 2013. Date of publication January 02, 2014; date of current version July 24, 2014. This work was founded by the U.S. National Science Foundation (NSF) Grant 1057644 and Grant CCF-1117545, by the Army Research Office under Grant 60219-MA, and by the Office of Naval Research under Grant N000141210765. This paper was recommended by Associate Editor M. Sawan.

J. Zhang, Y. Suo, S. P. Chin, T. D. Tran, and R. Etienne-Cummings are with the Department of Electrical and Computer Engineering, The Johns Hopkins University, Baltimore, MD 21218 USA (e-mail: jzhang41@jhu.edu).

S. Mitra and R. F. Yazicioglu are with imec, B-3001 Heverlee, Belgium.

S. Hsiao is with the Department of Neuroscience, The Johns Hopkins University, Baltimore, MD 21218 USA.

Color versions of one or more of the figures in this paper are available online at http://ieeexplore.ieee.org.

Digital Object Identifier 10.1109/TBCAS.2013.2284254

C. Summary of Our Paper's Contributions and Structure

However, despite many advantages of CS based systems, previous approaches failed to achieve impressive compression rate while maintaining high signal recovery quality, especially when a significant amount of noise is introduced to the neural signal [12].

In this paper, we improve upon previous CS systems in two aspects: 1) designing a signal dependent sparse representation and 2) adopting a model-based sparse recovery method based on prior signals. It is widely accepted in the field of Neuroscience that information in the brain is transmitted by occurrences of spikes. Each neuron's spike has a characteristic shape depending on its morphology and proximity to the recording electrode. This unique shape can be used to cluster and sort the spikes to their corresponding neuron [13]–[15]. Utilizing the same property, a signal dependent representation basis (also known as representation dictionary) could be trained from prior information of the spike to sparsely represent future recorded spikes.

We have introduced this approach in [16] with preliminary simulations results. In this paper, we first present a rigorous analysis and compare the proposed approach performance with other state of art compression methods mentioned in the Introduction. Then we discuss the considerations and trade-offs of an implementation of the proposed approach. Through measurements on a test-chip we conclude that the proposed approach can be implemented in an area of 200 × 300 μm, while consuming only 0.27 μW in a TSMC 0.18 μm process with VDD of 0.6 V.

The paper is divided into the following sections: the background knowledge is reviewed in Section II. The proposed signal reconstruction framework is described in Section III. Evaluation of the the proposed approach performance is presented in Section IV. Some non-ideality that the proposed system might face during real recording experiments is discussed in Section V. The design concepts of a neural signal compression system based on the proposed framework is addressed in Section VI, together with measurement results of an implemented test structure. Finally, conclusion and future work are presented in Section VII.

II. Background

A. Compressed Sensing

Compressed sensing was introduced as a theoretical framework regarding the exact recovery of an S-sparse signal $\mathbf{x}$ of length N from a measurement vector $\mathbf{y}$ of length M, where $S < M \ll N$. The S-sparse signal is defined as a signal that has exactly S non-zero coefficients in the entire length of N, or can be well approximated by its largest S coefficients.

Given that a sensing matrix A satisfies the Restricted Isometry Property (RIP) and $M \sim Slog(N/S)$ [17], [18], S-sparse vector $\mathbf{x}$ can be recovered with high probability by solving the following ℓ_1-norm minimization problem:

$$\underset{\mathbf{x}}{\operatorname{argmin}} \|\mathbf{x}\|_1 \quad s.t.\ \mathbf{y} = \mathbf{A}\mathbf{x}. \tag{1}$$

To reduce the number of measurements M, the signal needs to be as sparse as possible. Therefore we need to find a basis to sparsely represent the target neural signal.

B. Sparse Representation

In general, the signal $\mathbf{x}$ is not sparse. But it has a sparse representation $\mathbf{v}$ with respect to a basis (or dictionary) $\mathbf{D}$. i.e., $\mathbf{x} = \mathbf{D}\mathbf{v}$ and $\mathbf{v}$ is an S-sparse vector. Time-frequency transformations such as wavelet and Gabor frames are often used to represent the signal sparsely. However, analysis has shown that CS recovery using wavelets basis can only achieve compression rate of around 2:1 before recovery quality from the compressed samples becomes intolerable [12]. To increase the neural signal representation sparsity, we seek to train a signal dependent representation dictionary using the shapes of previously detected neural signals.

C. Dictionary Learning

Given a set of L training signal $\mathbf{X} = \{\mathbf{x_{i\,i=1}^{L}}\}$, where $\mathbf{x_i} \in \mathbf{R^N}$, the process of building a signal dependent dictionary is to solve the following optimization problem:

$$\underset{D,\{v_i\}_{i=1}^{L}}{\operatorname{argmin}} \sum_{i=1}^{L} \|\mathbf{x}_i - \mathbf{D}\mathbf{v}_i\|_2^2 \quad s.t. \|\mathbf{v}_i\|_0 \le s_0, 1 \le i \le L \tag{2}$$

where $\mathbf{D} \in \mathbf{R^{N \times P}}$ is the signal dependent dictionary. P denotes the size of the dictionary and $\mathbf{v}_i \in \mathbf{R^P}$ is the sparse vector representing the training data $\mathbf{x}_i$ in $\mathbf{D}$. s_0 is the bound on the ℓ_0-norm of the sparse vector.

Several dictionary learning algorithms were proposed to solve (2) [19]–[22]. Among these algorithms, we choose K-SVD [22] as the dictionary learning algorithm, which is inspired by the well known K-means. This algorithm is attractive as it has simple training steps and forms dictionary atoms that can be intuitively interpreted by the users. Note that the K-SVD algorithm becomes K-means if the sparsity s_0 is equals to 1 and the number of columns in the dictionary is equal to the number of spike classes.

III. Signal Representation and Recovery Framework

In this section, we present the framework to represent and recover the spike signals using signal dependent representations. We name this approach Signal Dependent Neural Compressed Sensing Method (SDNCS).

A. Dictionary Training

Using K-SVD algorithm, we first train a sparse representation dictionary $\mathbf{D}$ from training spike signals collected by the electrode. $\mathbf{D}$'s structure is directly related to the length of signal segment and the number of detected spike classes of an electrode. If the electrode detects K different spike classes, the trained dictionary $\mathbf{D}$ would be composed of sub-dictionaries $\{\mathbf{D}_{1,1}\,\mathbf{D}_{1,2}\ldots\mathbf{D}_{k,n}\}_{k=1\,n=1}^{K\,N}$, where N is the length of the signal segment. Each sub-dictionary, $\mathbf{D}_{k,n}$, contains atoms

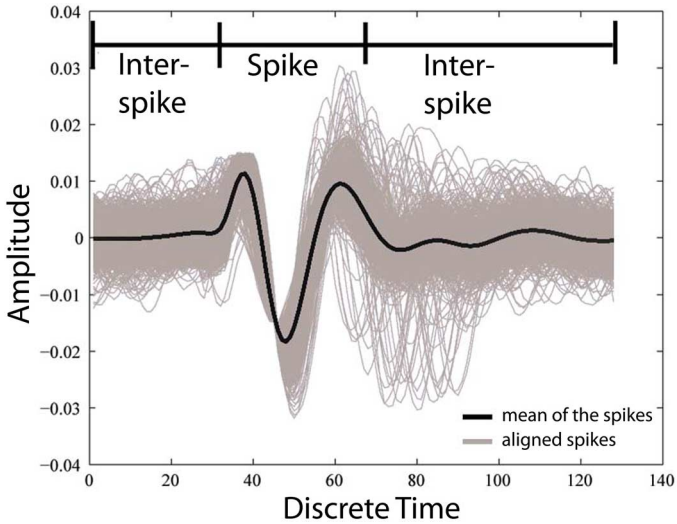

Fig. 1. Many spikes segments from one neuron aligned at its threshold crossing point. Grey traces are the spikes. The black trace is the mean of these spike frames, which can be used to sparsely represent the spikes.

representing kth spike class at temporal location n trained with sparsity of s_0.

The parameter s_0 determines the signal sparsity when they are represented by the dictionary. The smaller the s_0, the fewer number of measurements needed for exact signal recovery in the CS framework. Typical signal segments containing spikes look like the ones shown in Fig. 1 after they are aligned at a threshold crossing point. To seek a sparse representation of these spikes, the most obvious choice for an atom is the mean of the signals, shown as the black waveform placed on top of the spikes. In this case, $s_0 = 1$, and the K-SVD algorithm becomes K-mean algorithm. However, the inter-spike signals have a mean of almost zero, as demonstrated in Fig. 1. Therefore, if we choose $s_0 = 1$ in constructing the dictionary $\mathbf{D}$, the energy in the spike can be well represented at a cost of poor representation of the inter-spike signal. To address this trade-off, we seek to represent the band-limited inter-spike signal using standard time-frequency dictionaries, such as the discrete wavelet transform (DWT).

B. Recovery Framework

A spike signal, $\mathbf{x}$, can be decomposed as

$$\mathbf{x} = \mathbf{x}_c + \mathbf{x}_f \tag{3}$$

where $\mathbf{x}_c$ is a coarse estimation of the spike signal and $\mathbf{x}_f$ is the fine detailed estimation representing the difference between $\mathbf{x}$ and $\mathbf{x}_c$. Here $\mathbf{x}_c$ can be further represented in the trained dictionary $\mathbf{D}$ as a sparse vector $\mathbf{v}_c$ with sparsity s_0 of 1, such that $\mathbf{x}_c = \mathbf{D}\mathbf{v}_c$. When the spike's temporal duration is small relative to signal's temporal duration, the $\mathbf{x}_f$ term would be dominated by the energy of the inter-spike signal as labeled in Fig. 1. Due to its wavelike nature, $\mathbf{x}_f$ can be represented in a wavelet basis by a sparse vector $\mathbf{v}_f$, such that $\mathbf{x}_f = \mathbf{W}^{-1}\mathbf{v}_f$,

Definition:
$\boldsymbol{y}$: Compressed Sensing measurements; further decomposed into $\boldsymbol{y_c}$ and $\boldsymbol{y_f}$
$\boldsymbol{x}$: Spike signal segment; further decomposed into $\boldsymbol{x_c}$ and $\boldsymbol{x_f}$
$\boldsymbol{v}$: Sparse representation of $\boldsymbol{x}$; further decomposed into $\boldsymbol{v_c}$ and $\boldsymbol{v_f}$
$\boldsymbol{A}$: Sensing Matrix
$\boldsymbol{D}$: Trained sparse representation dictionary
$\boldsymbol{W^{-1}}$: Inverse Wavelet Transform basis
N: Length of signal $\boldsymbol{x}$

Training Stage
1. From the training data, identify the number of different spikes classes, K.
2. For j=1:K and i=1:N
   Train a sub-dictionary $\boldsymbol{D_{ij}}$ representing the i th spike class at j th temporal location with sparsity s_0 of one.
3. Form representation dictionary $\boldsymbol{D} = \{\boldsymbol{D_{ij}}\}_{i=1\,j=1}^{K\quad N}$

Recovery Stage
1. Compute estimator $\hat{\boldsymbol{v}}_c$, by solving:

$$\hat{\boldsymbol{v}}_c = argmin_{\boldsymbol{v_c}} \|\boldsymbol{y} - \boldsymbol{AD}\|_2 \quad s.t.\ \|\boldsymbol{v_c}\|_0 = s_0$$

2. Compute $\boldsymbol{y_{res}}$ by computing:

$$\boldsymbol{y_{res}} = \boldsymbol{y} - \boldsymbol{AD}\hat{\boldsymbol{v}}_c$$

3. Compute estimator $\hat{\boldsymbol{v}}_f$ by solving:

$$\hat{\boldsymbol{v}}_f = argmin_{\boldsymbol{v_f}} \|\boldsymbol{y_{res}} - \boldsymbol{AW^{-1}v_f}\|_2^2 \quad \boldsymbol{v_f} s.t. \quad \boldsymbol{v_f} \le \boldsymbol{\lambda}$$

4. Compute estimator $\hat{\boldsymbol{x}}$ by computing:

$$\hat{\boldsymbol{x}} = \boldsymbol{D}\hat{\boldsymbol{v}}_c + \boldsymbol{W^{-1}v_f}$$

Fig. 2. The proposed Signal Dependent Neural Compressed Sensing (SDNCS) approach.

where $\mathbf{W}^{-1}$ is the Inverse Discrete Wavelet Dictionary. The grey trace in Fig. 3(B.i) and (B.ii) shows an example of $\mathbf{x}_f$ in time domain and its sparse representation $\mathbf{v}_f$ in Daubechies-12 wavelets domain.

The proposed framework first utilizes the signal dependent dictionary to find $\mathbf{v}_c$ from the compressed measurements $\mathbf{y}$. Then it approximates the finer details representation term $\mathbf{v}_f$ using sparse representation in wavelet dictionaries. To begin the recovery, we first decompose CS measurements, $\mathbf{y}$, following the same method:

$$\mathbf{y} = \mathbf{y}_c + \mathbf{y}_f \tag{4}$$

where $\mathbf{y}_c$ is the CS measurements corresponding to $\mathbf{v}_c$. And $\mathbf{y}_f$ is the CS measuremnts of the $\mathbf{x}_f$ such that

$$\mathbf{y} = \mathbf{A}\mathbf{D}\mathbf{v}_c + \mathbf{A}\mathbf{W}^{-1}\mathbf{v}_f \tag{5}$$

where $\mathbf{A}$ is the random Bernoulli sensing matrix [17]. This framework essentially represent the signal using two different sparse representations. Therefore, in the recovery steps we first compute for $\hat{\mathbf{v}}_c$, an estimator to $\mathbf{v}_c$ represented in dictionary $\mathbf{D}$ by solving the following minimization problem:

$$\hat{\mathbf{v}}_c = \underset{\mathbf{v}_c}{\operatorname{argmin}} \|\mathbf{y} - \mathbf{A}\mathbf{D}\mathbf{v}_c\|_2^2 \quad s.t.\ \|\mathbf{v}_c\|_0 = s_0. \tag{6}$$

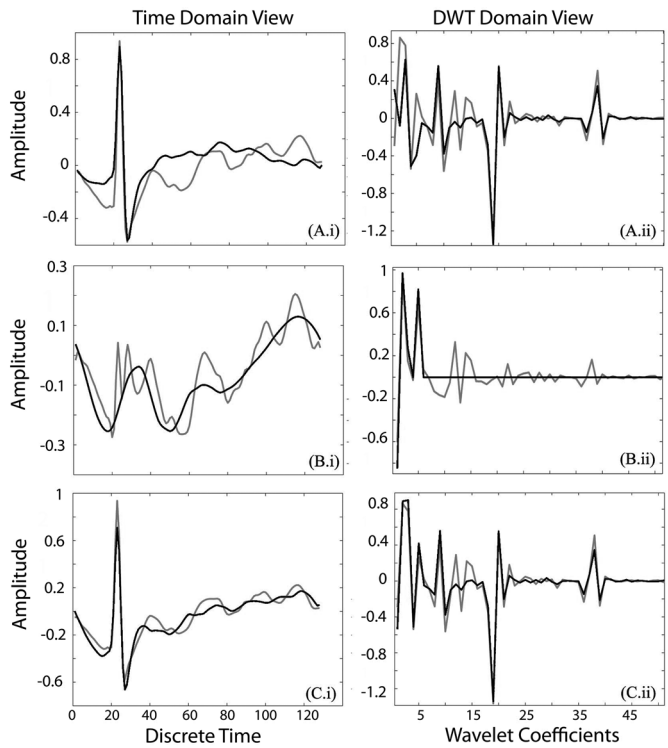

Fig. 3. Illustration of the proposed SDNCS approach. (A.i, A.ii) Temporal and DWT domain view of the coarse estimation $\hat{\mathbf{x}}_c$ (black trace) and original signal $\mathbf{x}$ (grey trace). (B.i, B.ii) Detail estimation $\hat{\mathbf{x}}_f$ (black trace) and $\mathbf{x}_f$ (grey trace). (C.i, C.ii) The signal estimation $\hat{\mathbf{x}}$ (black trace) and original signal $\mathbf{x}$ (grey trace).

The method to solve (6) is discussed in the following subsection. After finding $\hat{\mathbf{v}}_c$, it is projected back onto the sensing matrix $\mathbf{A}$ to find a residual $\mathbf{y}_{res}$ defined by

$$\mathbf{y}_{res} = \mathbf{y} - \mathbf{A}\mathbf{D}\hat{\mathbf{v}}_c. \tag{7}$$

Next, $\hat{\mathbf{v}}_f$, an estimator of $\mathbf{v}_f$ is then computed by solving the ℓ_1-minimization problem

$$\hat{\mathbf{v}}_f = \underset{\mathbf{v}_f}{\operatorname{argmin}} \|\mathbf{y}_{res} - \mathbf{A}\mathbf{W}^{-1}\mathbf{v}_f\|_2^2 \quad s.t.\ \|\mathbf{v}_f\|_1 \leq \lambda \tag{8}$$

where λ is the regularization parameter that balances the trade-off between data fidelity and sparsity. Many algorithms are available to solve (8). We choose a wavelet tree model based Compressive Sampling Matching Pursuit (CoSAMP) approach [23], as our simulation shows that it provides the best trade off between reconstruction quality and computation speed.

After finding $\hat{\mathbf{v}}_c$ and $\hat{\mathbf{v}}_v$, we combine them in (9) to find the estimation for the signal $\hat{\mathbf{x}}$ as follows:

$$\hat{\mathbf{x}} = \mathbf{D}\hat{\mathbf{v}}_c + \mathbf{W}^{-1}\hat{\mathbf{v}}_f. \tag{9}$$

The proposed SDNCS approach is summarized in Fig. 2. In addition we provide some graphical illustrations of the shapes of recovered signals at each stage of the recovery framework in Fig. 3.

C. Model Based Recovery Approach Using On-Chip Spike Detection Circuit

Greedy algorithms such as Orthogonal Matching Pursuit (OMP) [24] is chosen to solve the minimization problem in (6). For a signal containing a spike belonging to spike class k at temporal location n, OMP finds the atom in dictionary $\mathbf{D}$ that minimizes (6). The selected atom should belong to the sub-dictionary $\mathbf{D}_{k,n}$ so that the target spike can be reconstructed with high accuracy at the correct temporal location. However, when recording channel are corrupted by a high level of noise, OMP becomes more prone to select the wrong atom in reconstruction.

To improve the reconstruction quality, we propose a model based recovery approach utilizing the implementation of a simple on-chip spike detection circuit. This approach is motivated by the model based recovery approach discussed in [23]. On-chip spike detection circuit is able to relay the temporal location information of the spike to the recovery algorithm. For a spike occurring at temporal location i, instead of searching within dictionary $\mathbf{D}$, OMP algorithm searches through a much smaller set of atoms belonging to sub-dictionary $\{\mathbf{D}_{k,n}\}_{k=1}^{K}$ for the correct atom. Thus the greedy algorithm is more likely to converge on the global minimal solution instead of a local one. We name the model based approach as Signal Dependent Neural Compressed Sensing approach with Prior recovery information (SDNCS-P). Its performance is also validated in the next section of the paper.

IV. Reconstruction Quality Comparison

In this section, we present simulations results to compare the spike recovery quality and classification performance of the proposed algorithm with other state of the art compression methods mentioned in the introduction section. We also compare the hardware cost of each compression algorithm. Finally, we evaluate and compare the clustering performance of the proposed approach with results from a previous evaluation study [12] in situations when spike signal are corrupted by various amount of noise.

A. Recovery and Classification Quality Comparison

1) Data Description: Sample signals from University of Leicester neural signal database [25] are used to construct simulation experiment to evaluate the recovery performance of the proposed approach. Three different pieces of neural signals from the database are used in this evaluation experiment, denoted as Easy1, Easy2 and Hard1. The naming of the signals is consistent with that of the dataset [25]. As described in [15], these simulated signals contain spikes from 3 different neurons sampled at 24 KHz. To simplify experiment, we retained signal segments containing only one spike. Out of the 2046 spike signal frames extracted from this piece of neural signal, 20% of them are used to train the signal dependent dictionary, while the remaining 80% are used for testing and evaluation. We varied the number of training signal used in training the dictionary and have not observed significant change in results.

The temporal shapes of the test signals are shown in the top row of Fig. 4. Easy1 and Easy2 contains spike shapes having large temporal variance, while the Hard1 contains spike shapes that are very similar in the temporal domain.

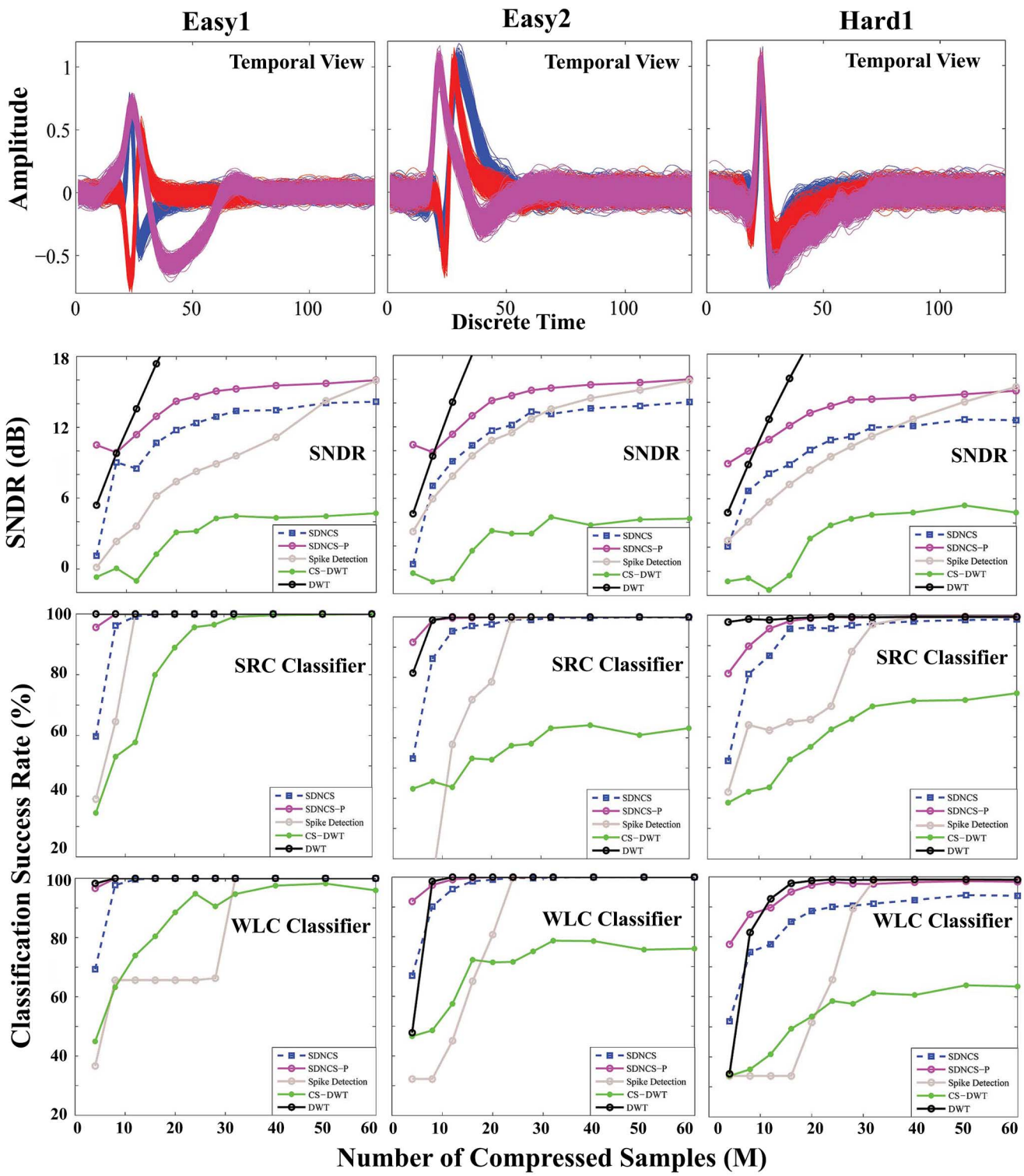

Fig. 4. Test signals' temporal views (top row) and recovery SNDR (2nd row) and classification quality (3rd and 4th row) comparison of Spike Detection, DWT, CS-DWT, SDNCS and SDNCS-P. In the plot of recovery SNDR, the window is set to display values in the range of −2 to 18 dB. The SNDR of DWT method increase beyond this range and approaches infinity as the number of M increases.

2) Experiment Setup: In the simulation, each signal frame has discrete length $N = 128$, which contains duration of signal of around 5.3 ms, more than twice in temporal duration of a typical spike signal (around 2 ms). The test signals are compressed to a vector of length M after mixing with a $M \times N$ sensing matrix, where $M \ll N$. A Random i.i.d Bernoulli matrix is chosen as the sensing matrix because it guarantees excellent reconstruction quality and implementation efficiency [1]. All test signals are compressed and reconstructed 30 times, using a different sensing matrix in each trial. The results are then averaged across all trials.

The recovery quality of the SDNCS and SDNCS-P methods are compared with other compression methods mentioned in the Introduction of the paper. They are: Spike detection and windowing [2], [3], Wavelet transformed and thresholding (DWT) [7], [8] and Compressed Sensing with recovery using only wavelet basis (CS-DWT) [9]–[11]. In the spike detection and windowing method, M samples are kept around a threshold crossing location while other samples of the signal are discarded. In the DWT compression method, the signal is first transformed into wavelet representation and M most significant coefficients are retained to represent the signal. In the CS-DWT compression method, the signal is mixed with the sensing matrix to obtain a compressed vector of length M, which is then recovered using wavelet transform basis.

3) Evaluation Metrics: Signal to Noise and Distortion Ratio (SNDR) is used as a metric [1], [10] to evaluate recovery quality. SNDR is defined as

$$\mathrm{SNDR} = 20 \log \frac{\|\mathbf{x}\|_2}{\|\mathbf{x} - \hat{\mathbf{x}}\|_2}. \tag{10}$$

SNDR as defined here is a metric to measure the reconstruction quality. It should not be confused with signal SNDR at the front end of the recording circuit or that of the ADC.

Spike classification successful rate is also used as a performance metric, calculated as a percentage of total number of spikes correctly classified. After the signal is reconstructed from the compressed measurements, it is classified using spike classifiers. The classification results are compared with the ground truth labels contained in the database. Two different types of spike classifiers were used to minimize comparison biases related to classifiers. One of the them is a wavelet based classifier (WLC) [15] widely used in spike sorting applications. The other one is a sparse representation classifier (SRC) proposed in [26].

4) Results: The experiment results are shown in Fig. 4. From the SNDR comparison, both the SDNCS and SDNCS-P consistently outperform CS-DWT method by around 8–10 dB. They also outperforms Spike Detection method at high compression rate (i.e., when M is low).

However, the DWT approach outperforms the other methods by a significant margin in term of recovery SNDR. This is expected as the number of DWT samples increase, the recovered signal is able to exactly match even the finer details of the original signal. But in term of spike classification accuracy, the SDNCS-P's performance is comparable to that of DWT method. Fig. 5 demonstrates two reconstructed signals' temporal view. Although they have different SNDR, the spike part of the signal is well reconstructed.

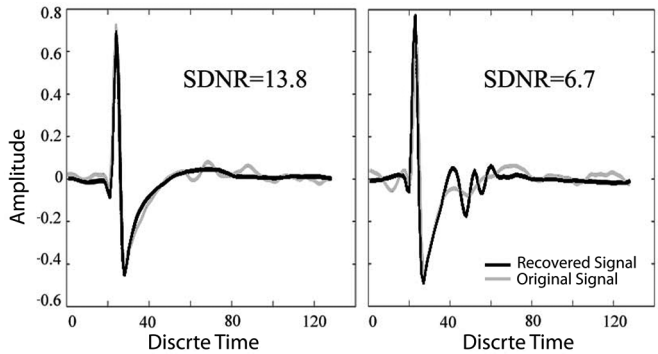

Fig. 5. Recovered signals with different SNDR (black) recovered signal (grey) original signal. Mismatch of the recovered signal with the original signal around the spike causes significant degradation to recovery SNDR, despite the shape is well recovered.

B. Hardware Cost Comparison

1) Data Description: Noise corrupted version of Easy1, Easy2 and Hard1 signal are used in this experiment. These signals have normalized mean of 1 and corrupted by various amount noise having standard deviation of 0.05 to 0.2.

2) Experiment Setup: This experiment evaluates the hardware cost of different comparison methods in order to achieve the same reconstruction performance. The signals are compressed and recovered using the methods described in the previous subsection. For all three algorithms under comparison, the value of M, the number of compressed samples required for classification accuracy to reach above 90% is recorded.

3) Evaluation Metrics: The hardware cost is compared through a Hardware Figure of Merit (FOM) defined as

$$\mathrm{FOM} = Transmission\ power \times Circuit\ Area \times Circuit\ speed. \tag{11}$$

The transmission power cost depends on many factors such as desired communication distance, transmission media and wireless circuit architectures. Thus, it is difficult to compute a meaningful numerical value to represent the transmission power cost without making an overwhelming number of assumptions. However, the transmission power is always proportional to the data volume. Therefore we simply use the number of compressed sample M to represent transmission power.

We choose the number of transistors in the circuit as the metric to represent the circuit area. All of the compression methods are implemented using digital circuits. Therefore, the number of transistors in the circuit is directly proportional to the circuit layout area.

Finally, the circuit clock frequency is a direct measure of the circuit operating speed, which reflects the circuit's computational power. The operating speed can also be presented as a ratio with the neural signal's Nyquist frequency [7].

Thus, the FOM can be rewritten as

$$\mathrm{FOM} = Trans.\ count \times \frac{Clock\ Freq.}{Nyquist\ Freq.} \times M \times \frac{1}{100}. \tag{12}$$

The $(1)/(100)$ is a scaling factor to prevent the numerical value of the FOM become too large for comparison. This scaling factor is common to all the compression methods, so it would not alter the comparison of Figure of Merit (FOM).

To estimate transistor count and circuit operating frequency for different compression methods, we assume each incoming neural signal sample has 10-bits resolution. The Spike Detection method therefore requires the implementation of a 10-bits

digital comparator operating at signal Nyquist rate. A 10 bits ripple adder with 10 bits registers can be used to construct this comparator due to its low required operation speed. If one full adder consists of 28 transistors [27] and one master-slave edge triggered register has 20 transistors [28], the 10 bits adder-register pair would have 480 transistors. Additionally, windowing method requires FIFO to buffer the samples before a threshold crossing event [6], [3]. The buffer is chosen to store 15 samples of spike prior to threshold crossing event, corresponding to 30% of a spike with temporal duration of 2 ms sampled at 25 KHz [6]. If buffers are constructed using registers, then 15 10-bit registers contains 3000 transistors. Hence, the spike detection method has transistor count of 3480, operating at signal Nyquist Frequency.

The compressed sensing circuits requires parallel accumulators for the random mixing operation. To account for overflow, 13 bits accumulators implemented with registers and full-adders are required. Thus, each accumulator consists of 624 transistors. The CS system transistor count scales with compression rate as unused accumulators can be turned off by clock gating. CS-DWT method and SDNCS method have identical hardware, while SDNCS-P requires extra implementation of a 10 bit digital comparator before CS mixing circuits.

An on-chip implementation of a 7 level discrete wavelet transform unit requires 12508 total number of transistors according to the specifications given in [7]. Furthermore, the system operates at a frequency around two times higher than the signal Nyquist rate.

4) Results: From the results obtained in Fig. 6, the SDNCS and SDNCS-P algorithms outperform both CS-DWT and Spike Detection across all noise level in terms of number of samples required to reach 90% classification accuracy. The SDNCS-P method has comparable compression rate as DWT method at low noise level. But it requires more samples to reach 90% classification accuracy than DWT method at high noise level.

In term of FOM, SDNCS-P outperforms other methods by orders of magnitude except at signal Easy2 with noise standard deviation of 0.15, where the Spike Detection method outperforms SDNCS-P marginally. However, the compression rate of SDNCS-P is still around two times higher than that of the Spike Detection Method.

C. Spike Clustering Quality Across Different Noise Level.

1) Data Description: Noise corrupted versions of Easy1 signal from the Leicester database [25] are used in the clustering experiment. These signals have normalized spike amplitude of 1 and corrupted by various amount of noise having standard deviation from 0.05 to 0.4. This signal is also used in the CS clustering performance evaluation study outlined in [12].

2) Experiment Setup: Each signal is divided into training section and test section, composed with 20% and 80% of the signal. Using training dataset, we first determine the spike clusters using Osort [29] online cluster software. A sparse representation dictionary is then constructed.

We replicated the experiment setup in [12] to compare spike clustering performance across different noise levels. The signal is first quantized into 8-bits digital resolution. After quantization, the uncompressed test data is processed by Osort to establish a baseline clustering results. The test signal is then passed through a power based spike detector implemented within Osort algorithm before it is compressed using an M $\times$ N sensing matrix, where $N = 128$. The signal is recovered using SDNCS-P approach and processed using Osort to determine the clustering result of the recovery signal.

3) Evaluation Metrics: The metric used to determine clustering performance is the percentage of correctly assigned spikes. It measures the percentage of spikes in baseline clusters that is also correctly assigned to the same clusters after compression and recovery. Percentage of correctly assigned spikes under different noise level and compression rate is plotted against the signal Compression Rate (CR) in Fig. 7, where $\mathrm{CR} = (N)/(M)$. As a comparison, the results from the dictionary learning CS approach outlined in [12] is also plotted in 7.

4) Results: As compression rate and noise increases, the SDNCS-P performance still maintains high clustering accuracy above 85%, whereas the previous dictionary learning CS approach outlined in [12] achieves clustering accuracy of around 20%. Fig. 7(b), (c) also shows a time domain view of the reconstructed spikes under different compression rate when noise standard deviation is 0.4.

V. Non-Ideality Considerations

The proposed algorithm is evaluated using synthesized dataset in this paper. However, in a real neural recording experiment, several non-ideal situations might also arise:

A. Spike Occurrence Within a Signal Frame

First of all, since the purposed recovery method is signal dependent, it is essential for the system to detect the occurrence of spike within each signal frame. If a signal frame contains no spike, then it would be inappropriate to use a signal dependent dictionary to reconstruct this frame. Instead, this frame should be reconstructed using a standard time-frequency basis.

Secondly, a signal frame may contain two or more spikes and they might be super-positioned on top of each other, resulting in a large spike. For example, In the signal frames shown in Fig. 8, there exist two spike signals in a single frame. In the first case, two spikes are separated in time. In the second case, two spikes are super-positioned on top of each other so that it looks like one large spike. The proposed dictionary based CS recovery might encounter difficulty in recovering these frame if only a single dictionary atom is used for reconstruction. However, on-chip detection circuit could relay these non-ideal information to the recovery algorithm. For example, two threshold levels can be set, showing as a horizontal black lines in Fig. 8. In the first case, the spikes crosses the lower threshold twice, and in the second case, the spikes crosses both thresholds. Using these detected evidences, the on chip system could signal the off-chip recovery algorithms to attempt to recover these signal frames by using two dictionary atoms, belonging to two different spike classes. The black traces in Fig. 8 are the recovered results using two atoms from the trained dictionary. With the extra information,

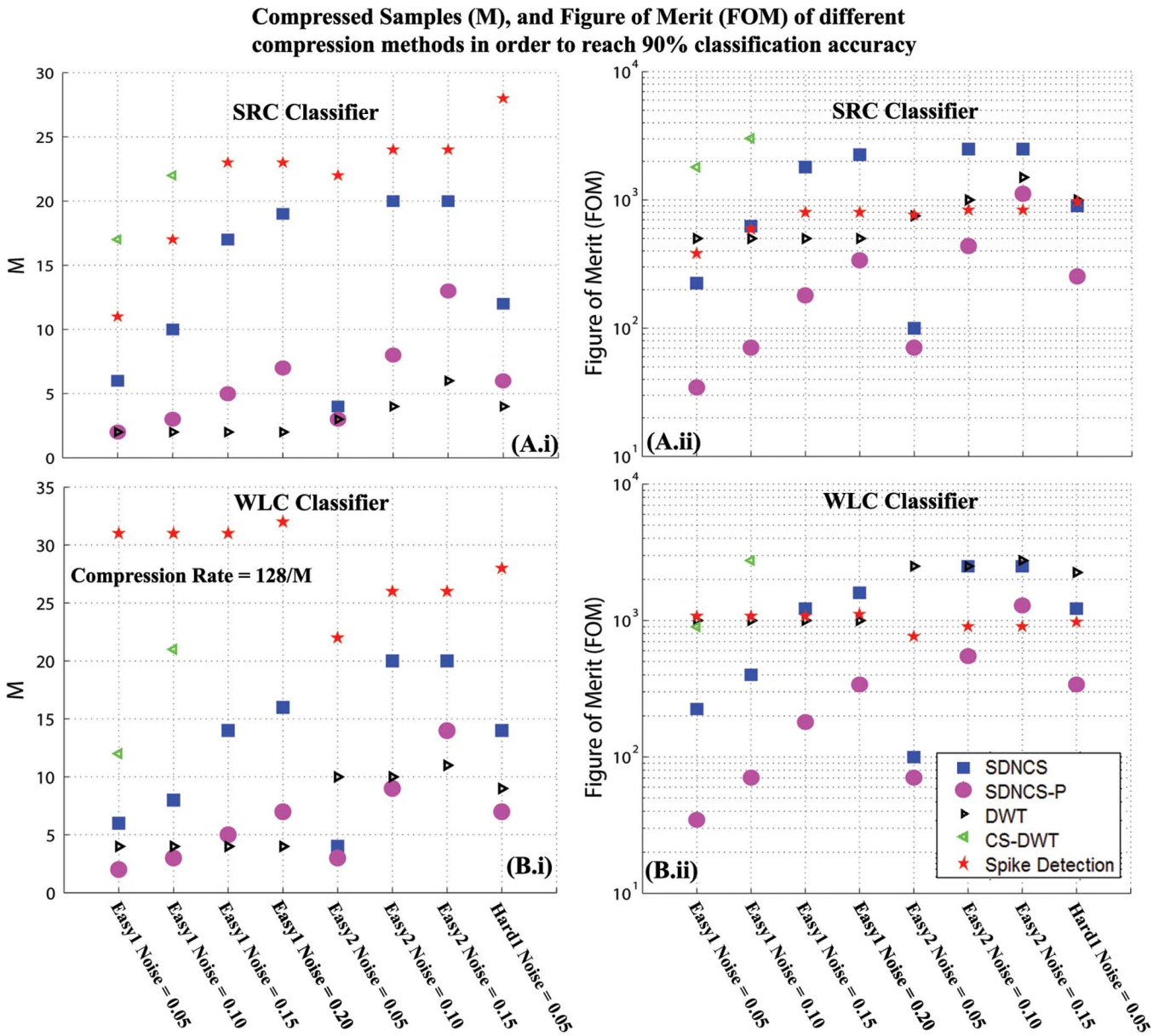

Fig. 6. Figures showing number of compressed samples (M) and Figure of Merit (FOM) of different compression method in order to achieve 90% classification accuracy under both SRC (Subfigure A.i and A.ii) and WLC classifier (Subfigure B.i and B.ii). Points are omitted from the plot when a compression method never reach 90% classification accuracy.

the proposed SDNCS and SDNCS-P approaches successfully reconstructs multiple spikes in the signal frame.

B. Signal Degradation or Variation Over Time

Although the neuron's action potentials shapes exhibits excellent invariability over time, these spike shapes might still vary under some circumstances, such as movement of recording electrode. Over time, electrolysis in the recording area might also induce changes in electrode impedance, causing the recorded spike shapes to vary. Thus, the compression system must have feedback mechanism to detect the situation where a spike shape can no longer be described using the dictionary. Modifications on the off-chip spike classifiers can be made to compute the confidence level of each classification. When spikes are detected but fails to be classified, the off-chip recovery system will signal the on-chip compression system to transmit raw recording to learn a new dictionary.

VI. System Design Concepts

In this section, we propose a CS system based on the SDNCS and SDNCS-P approach. A block diagram of the system is shown in Fig. 9 in relations with other components of a typical neural recording circuit. Raw neural signal is first conditioned into appropriate bandwidth and amplitude using on-chip amplifier and band pass filter. Analog to Digital Converter (ADC) then digitizes the signal at its Nyquist rate. Before the CS compression system is activated, the recorded raw signals are sent off-chip so that a dictionary can be trained off-chip. Base on the raw recording, the user can also configure the optimal threshold to use for spike detection. After the dictionary is successfully

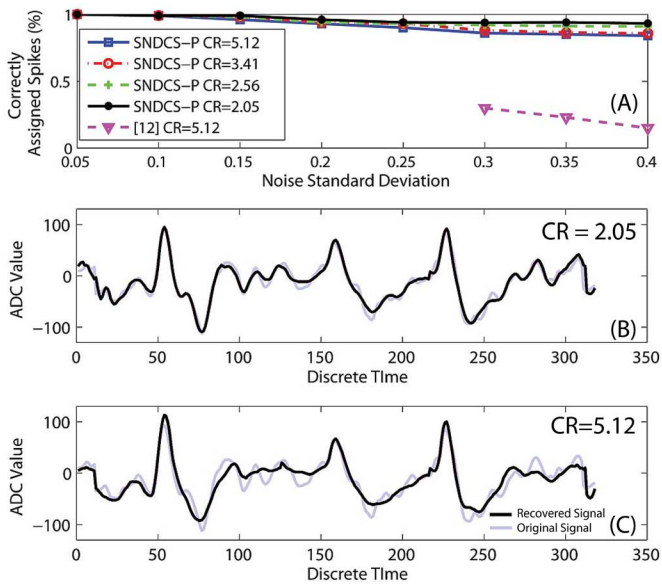

Fig. 7. (a) Correctly Assigned Spikes Percentage versus Noise Standard Deviation for various M. (b) and (c) Temporal view of the reconstructed signal (black trace) versus Original Signal (grey trace) when noise standard deviation is 0.4.

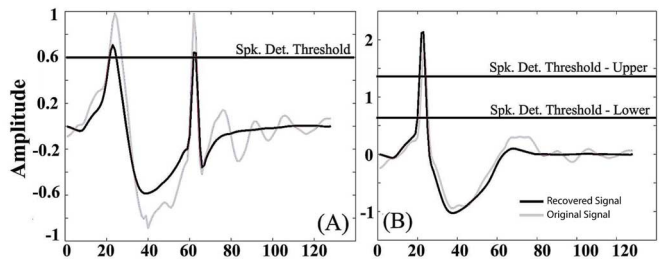

Fig. 8. (Grey trace) Original Signal (black trace) Recovered signal. (a) Situation when there are two spike detected in a single signal frame. (b) Situation when two spike fired at around the same time, results in a larger spike.

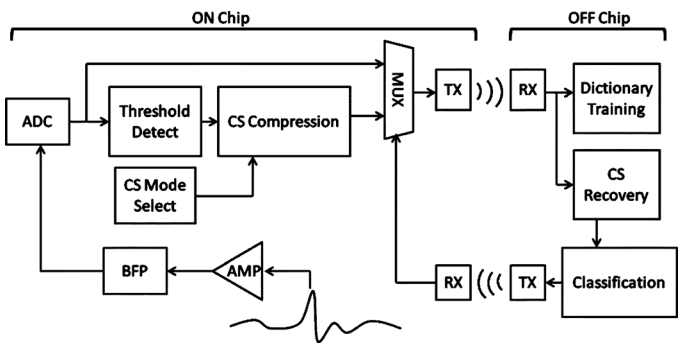

Fig. 9. Purposed System block diagram.

trained, the CS compressed system is activated to mix the output of the ADC with a random sensing matrix implemented using digital accumulators (Fig. 10). These accumulators were also referred to as CS Channels in previous works [1], [9]. The compressed measurements are transmitted off-chip via a wireless link. At the receiver's end, A CS recovery algorithm is running real time to reconstruct the signal and provide feedback to the on-chip sensing system if spikes are detected but failed

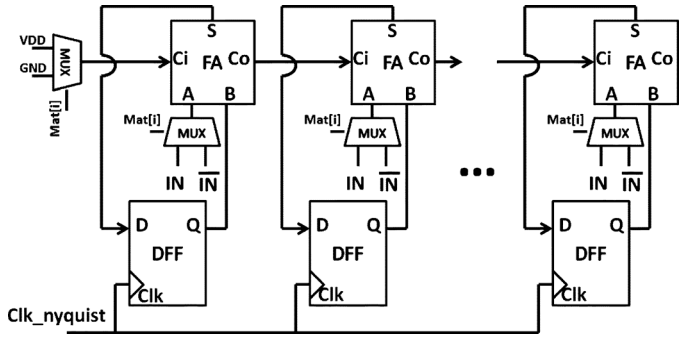

Fig. 10. The accumulator based design of the proposed CS channel.

to be classified. In the rest of this section, we discussed several key concepts regarding designing the proposed system.

A. Compressed Sensing Mixing Circuits

The CS Channels can be implemented using the accumulator circuit shown in Fig. 10. Depending on the value of Mat[i], the ith row of the sensing matrix $\mathbf{A}$, the accumulator may either add or subtract the incoming signal from the value already accumulated on it.

An alternative implementation of the CS Channel was shown in the previous works [1], [9]. Instead of using Bernoulli Random Matrix, this architecture implemented mixing operation of signal with a Random Binary Matrix. Instead of subtracting incoming value from the accumulated value, the CS Channel simply stay idle when the value of the matrix is a '0'. This implement could further reduce active power of the digital circuit, while not causing notable degradation in signal recovery quality. However, our simulation has shown that when the number of CS channel is small at high compression rate, we achieve better signal recovery quality using the Random Bernoulli Matrix compare to Binary Random Matrix.

The Random Sensing Matrix could be implemented using Linear Feedback Shift Registers (LFSR), proposed in [1]. It could also be implemented using on board registers or on-chip RAM, which would provide more flexibility in choosing the sensing matrix, as custom designed sensing matrix could decrease the dictionary mutual coherence and improve recovery quality [30], [31]. Register or RAM based implementation of sensing matrix is not efficient in terms of their layout area. But since many recording channels could share a single sensing matrix, an RAM or register based implementation might be preferable for high density electrode array to enhance recovery quality.

B. CS Subsystem Area and Power Consumption

The power consumption of the compressed sensing sub-system is dominated by the active power of the accumulator circuits. To estimate the power consumption, we have implemented test structures of the CS Channel on the TSMC 0.18 μm process. Fig. 11 shows the layout of this test chip with the accumulator and the ADC highlighted. This chip contains 100 CS channels implemented using the architecture proposed in [1]. The input of the CS channels are connected to a 10 bit SAR ADC operating at 20 KHz. As mentioned earlier, the

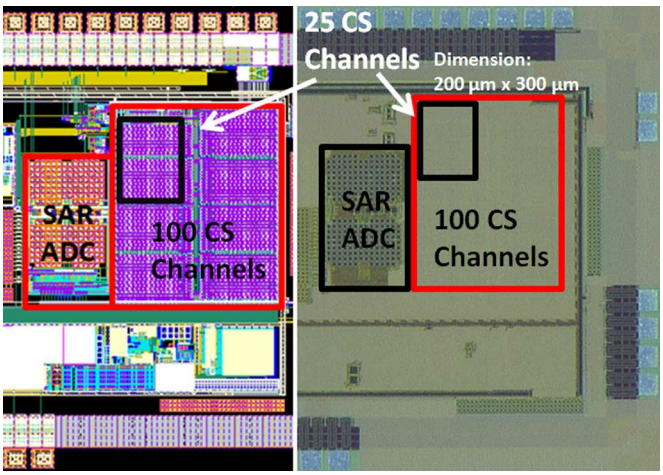

Fig. 11. Layout and micrograph of the chip in TSMC 0.18 μm process.

only difference of the test CS accumulator structure with the proposed structure is that the proposed structure implements a random Bernoulli sensing matrix with $+1/-1$ entry while the test structure implements a $+1/0$ random Binary sensing matrix.

From the results in Fig. 4, we observe that SDNCS reconstruction reaches the best performance around M of 15 to 20. Adding an over-design safe factor, 25 CS channels should be implemented for the proposed SDNCS system. 25 CS channels on the chip occupies an area of 200×300 μm, indicated by the small block box in Fig. 11. The measured total power consumption for 25 CS channel is 0.27 μW at 20 KHz sampling frequency when the VDD is at 0.6 V.

We have used pre-recorded neural signal from Primary Somatosensory cortex of the monkey to validate the performance of the implemented test structure. This signal is collected by The Somatosensory Lab at the Zanvyl Krieger Mind Brain Institute of the Johns Hopkins University. The recording setup is shown in Fig. 12(a). The classification accuracy, the temporal view of the pre-recorded signal, and a view of the reconstruction are also shown in Fig. 12.

VII. Conclusion and Future Work

A. Conclusion

In this paper, we present a signal dependent compressed sensing approach used to compress neural action potential before they are transmitted off-chip. Through simulation, we have demonstrated this approach outperformed signal independent compress sensing method and spike detection method in term of compression rate and recovery quality. The proposed approach achieves similar performance as DWT method, but requires far less complicated circuits components and power consumption. The simulations also illustrate the proposed framework's performance is robust under different noise level.

To summarize, our analysis using benchmark signals has shown that the proposed SDNCS could achieve compression rate from 8 to 16 while guarantee almost perfect spike classification rate. The compression circuit for a single recording electrode occupies area of 200 μ m $\times$ 300μ m and consumes

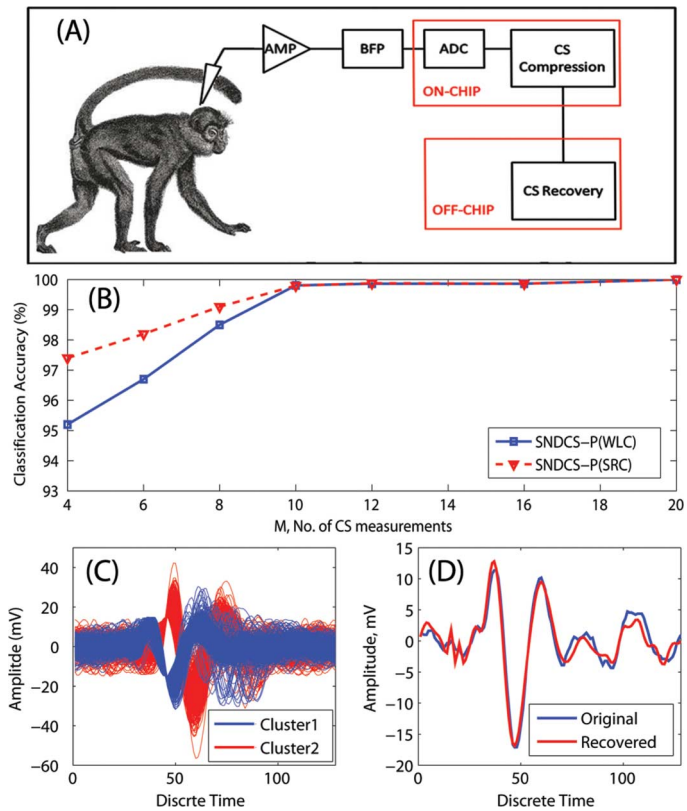

Fig. 12. (a) Illustration of the recording setup at the Primary Somatosensory Cortex of a monkey. (b) SDNCS-P Classification performance using test structure. (c) Temporal view of the pre-recorded signals. (d) Recovered signal using 25 on chip CS channels using SDNCS at VDD of 0.6 V versus Original signal.

0.27 μW at VDD of 0.6 V, making the system feasible for integration into high-density multi-electrodes neural recording arrays.

B. Future Work

The validation experiments in this paper are performed using synthesized dataset where major source of noise follows a Gaussian distribution. These experiments serve as a proof of concept verification. As we mentioned in Section VI, the real recording experiment may contain many non-ideal situations. A complete evaluation of the proposed algorithm and solutions for these non-ideal situation is our future work.

Acknowledgment

The authors would like to thank A. Cheng and Z. Lai from The Somatosensory Lab at the Zanvyl Krieger Mind Brain Institute of The Johns Hopkins University for providing us with real neural recordings.

References

[1] F. Chen, A. P. Chandrakasan, and V. M. Stojanovic, "Design and analysis of a hardware-efficient compressed sensing architecture for data compression in wireless sensors," *IEEE J. Solid-State Circuits*, vol. 47, no. 3, pp. 744–756, Mar. 2012.

[2] A. Rodriguez-Perez, J. Ruiz-Amaya, M. Delgado-Restituto, and A. Rodriguez-Vazquez, "A low-power programmable neural spike detection channel with embedded calibration and data compression," *IEEE Trans. Biomed. Circuits Syst.*, vol. 6, no. 2, pp. 87–100, Apr. 2012.

[3] S. Mitra, J. Putzeys, F. Battaglia, C. Mora Lopez, M. Welkenhuysen, C. Pennartz, C. Van Hoof, and F. Yazicioglu, "24-channel dual-band wireless neural recorder with activity-dependent power consumption," in *Proc. Int. Solid-State Circuits Conf.*, Feb. 2013, pp. 292–293.

[4] M. Chae, W. Liu, Z. Yang, T. Chen, J. Kim, M. Sivaprakasam, and M. Yuce, "A 128-channel 6 mw wireless neural recording IC with on-the-fly spike sorting and UWB transmitter," in *Proc. Solid-State Circuits Conf.*, 2008, pp. 146–603.

[5] B. Gosselin and M. Sawan, "An ultra low-power cmos automatic action potential detector," *IEEE Trans. Neural Syst. Rehabil. Eng.*, vol. 17, no. 4, pp. 346–353, Aug. 2009.

[6] B. Gosselin, A. E. Ayoub, J. F. Roy, M. Sawan, F. Lepore, A. Chaudhuri, and D. Guitton, "A mixed-signal multichip neural recording interface with bandwidth reduction," *IEEE Trans. Biomed. Circuits Syst.*, vol. 3, no. 3, pp. 129–141, Jun. 2009.

[7] K. G. Oweiss, A. Mason, Y. Suhail, A. M. Kamboh, and K. E. Thomson, "A scalable wavelet transform VLSI architecture for real-time signal processing in high-density intra-cortical implants," *IEEE Trans. Circuits Syst. I, Reg. Papers*, vol. 54, no. 6, pp. 1266–1278, Jun. 2007.

[8] A. M. Kamboh, A. Mason, and K. G. Oweiss, "Analysis of lifting and b-spline DWT implementations for implantable neuroprosthetics," *J. Signal Process. Syst.*, vol. 52, pp. 249–261, Sep. 2008.

[9] H. Mamaghanian, N. Khaled, D. Atienza, and P. Vandergheynst, "Compressed sensing for real-time energy-efficient ecg compression on wireless body sensor nodes," *IEEE Trans. Biomed. Eng.*, vol. 58, no. 9, pp. 2456–2466, Sep. 2011.

[10] A. M. R. Dixon, E. G. Allstot, D. Gangopadhyay, and D. J. Allstot, "Compressed sensing system considerations for ecg and emg wireless biosensors," *IEEE Trans. Biomed. Circuits Syst.*, vol. 6, no. 2, pp. 156–166, Apr. 2012.

[11] Z. Charbiwala, V. Karkare, S. Gibson, D. Markovic, and M. B. Srivastava, "Compressive sensing of neural action potentials using a learned union of supports," in *Proc. Int. Conf. Body Sensor Networks*, May 2011, pp. 53–58.

[12] C. Bulach, U. Bihr, and M. Ortmanns, "Evaluation study of compressed sensing for neural spike recordings," in *Proc. Annu. Int. Conf. IEEE Engineering in Medicine and Biology Soc.*, Sep. 2012, pp. 3507–3510.

[13] T. Sasaki, N. Matsuki, and Y. Ikegaya, "Action-potential modulation during axonal conduction. science signalling," *Sci. Signal.*, vol. 331, no. 6017, pp. 599–601, 2011.

[14] P. H. Thakur, H. Lu, S. S. Hsiao, and K. O. Johnson, "Automated optimal detection and classification of neural action potentials in extracellular recordings," *J. Neurosci. Methods*, vol. 162, pp. 364–376, May 2007.

[15] R. Q. Quiroga, Z. Nadasdy, and Y. Ben-Shaul, "Unsupervised spike detection and sorting with wavelets and superparamagnetic clustering," *Neural Comput.*, vol. 16, no. 8, pp. 1661–1687, Aug. 2004.

[16] J. Zhang, Y. Suo, S. Mitra, S. Chin, T. Tran, F. Yazicioglu, and R. Etienne-Cummings, "Reconstruction of neural action potentials using signal dependent sparse representations," in *Proc. IEEE Int. Symp. Circuits and Syst.*, May 19–24, 2001.

[17] E. Candes, J. Romberg, and T. Tao, "Robust uncertainty principles: Exact signal reconstruction from highly incomplete frequency information," *IEEE Trans. Inf. Theory*, vol. 52, no. 2, pp. 489–509, Feb. 2006.

[18] D. L. Donoho, "Compressed sensing," *IEEE Trans. Inf. Theory*, vol. 52, no. 4, pp. 1289–1306, Apr. 2006.

[19] M. S. Lewicki and B. A. Olshausen, "Probabilistic framework for the adaptation and comparison of image codes," *J. Opt. Soc. Amer. A*, vol. 16, no. 7, pp. 1587–160, 1999.

[20] M. S. Lewicki and T. J. Sejnowski, "Learning overcomplete representations. neural computation," *Neural Comput.*, vol. 12, no. 2, pp. 337–365, 2000.

[21] K. Engan, S. O. Aase, and J. H. Husoy, "Multi-frame compression: Theory and design," *Signal Process.*, vol. 80, 10, pp. 2121–2140, Oct. 2012.

[22] M. Aharon, M. Elad, and A. Bruckstein, "K-SVD: An algorithm for designing overcomplete dictionaries for sparse representation," *IEEE Trans. Signal Process.*, vol. 54, no. 11, pp. 4311–4322, Nov. 2006.

[23] R. G. Baraniuk, V. Cevher, M. F. Duarte, and C. Hegde, "Model-based compressive sensing," *IEEE Trans. Inf. Theory*, vol. 56, no. 4, pp. 1982–2001, Apr. 2010.

[24] J. A. Tropp, "Signal recovery from random measurements via orthogonal matching pursuit," *IEEE Trans. Inf. Theory*, vol. 53, no. 12, pp. 4655–4666, Dec. 2007.

[25] University of Leicester Neuroengineering Lab Website [Online]. Available: http://www2.le.ac.uk/departments/engineering/research/bioengineering/neuroengineering-lab

[26] J. Wright, A. Y. Yang, A. Ganesh, S. S. Sastry, and Y. Ma, "Robust face recognition via sparse representation," *IEEE Trans. Pattern Anal. Mach. Intell.*, vol. 31, no. 2, pp. 210–227, Feb. 2009.

[27] N. H. Weste and K. Eshraghian, *Principles of CMOS VLSI Design: A Systems Perspective*. Reading, MA, USA: Addison-Wesley, 1993.

[28] J. M. Rabaey, A. P. Chandrakasan, and B. Nikolic, *Digital Integrated Circuits*. Englewood Cliffs, NJ, USA: Prentice-Hall, 2002.

[29] U. Rutishauser, E. M. Schuman, and A. N. Mamelak, "Online detection and sorting of extracellularly recorded action potentials in human medial temporal lobe recordings, in vivo," *J. Neurosci. Methods*, vol. 154, pp. 204–224, Jun. 2006.

[30] M. Elad, "Optimized projections for compressed sensing," *IEEE Trans. Signal Process.*, vol. 55, no. 12, pp. 5695–5702, Dec. 2007.

[31] J. M. Duarte-Carvajalino and G. Sapiro, "Learning to sense sparse signals: Simultaneous sensing matrix and sparsifying dictionary optimization," *IEEE Trans. Image Process.*, vol. 18, no. 7, pp. 1395–1408, Jul. 2009.

Jie Zhang (S'11) received the B.Sc. degree in electrical engineering, from The Johns Hopkins University (JHU), Baltimore, MD, USA, in 2010.

Currently, he is working toward the Ph.D. degree in electrical engineering at JHU. He was an International Scholar with the Ultra Low Power—Biomedical Circuit Group at imec, Heverlee, Belgium, from October 2011 to July 2012. The focus of his research is compressive sensing, analog and mixed signal circuits design with low power biomedical applications.

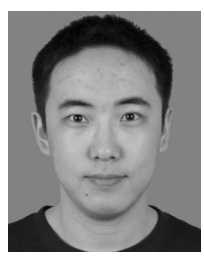

Yuanming Suo (S'11) received the B.S. degree in electronic information science and technology from Sun Yat-sen University, Guangdong, China, and the M.S.E. degree in electrical and computer engineering from the University of Alabama, Huntsville, AL, USA.

From 2004 to 2007, he was with China Netcom as a Computer Network Engineer. Currently, he is working toward the Ph.D. degree at The Johns Hopkins University, Baltimore, MD, USA, in the Digital Signal Processing Lab, where his research focuses on developing algorithms for dictionary learning, matrix completion and representations for high-dimensional data. His other research interests include image analysis in medical/remote sensing applications and compressed sensing.

Srinjoy Mitra (M'09) received the B.S. degree from the University of Calcutta, Kolkata, India, the M.Tech. degree from the Indian Institute of Technology, Bombay, India, and the Ph.D. degree from the Institute of Neuroinformatics, University of Zurich, ETH Zurich, Zurich, Switzerland.

He briefly worked in the microelectronic industry. He spent two years as a Postdoctoral Researcher at The Johns Hopkins University, Baltimore, MD, USA, and joined the medical electronics team at imec, Heverlee, Belgium, in 2010. His interests are in low-power analog circuits for biomedical interfaces.

Sang (Peter) Chin received the B.S. degree in electrical engineering, computer science, and mathematics from Duke University, Durham, NC, USA, and the Ph.D. degree in mathematics from the Massachusetts Institute of Technology, Cambridge, MA, USA, in 1993 and 1998, respectively.

Currently, he is a Research Professor in the Department of Electrical and Computer Engineering, The Johns Hopkins University (JHU), Baltimore, MD, USA, where he is conducting research in the area of compressive sensing, data fusion, game theory, MHT tracking, quantum-game inspired cyber-security, and cognitive radio. He is a PI for a four-year ONR grant (Geometric Multi-Resolution Analysis), applying geometric sparse recovery techniques to high dimensional data with low intrinsic dimension. Prior to joining JHU, he was a Division CTO at SAIC and worked on developing 90 nm technology at LSI Logic Corp., where he also helped to develop its first embedded DRAM technology jointly with Hitachi Semiconductor in the late 1990s.

Steven Hsiao received the B.S.E. degree from Duke University, Durham, NC, USA, and the Ph.D. degree from The Johns Hopkins University (JHU), Baltimore, MD, USA.

Currently, he is a Professor of neuroscience and biomedical engineering at JHU. He is a Neurophysiologist who studies the neural mechanisms of tactile perception. He is interested in understanding how texture and objects are represented in the cortex and the neural mechanisms of selective attention. In his studies, he records the responses of single neurons in the somatosensory system in animals and correlates those responses with behavior.

Refet Firat Yazicioglu (M'06) received the B.S. and M.S. degrees in electrical and electronics engineering from Middle East Technical University (METU), Ankara, Turkey, in 2001 and 2003, respectively, and the Ph.D. degree in electronics engineering, with an emphasis on the design of low-power and low-noise readout circuits for portable biopotential acquisition systems, from Katholieke Universiteit Leuven, Leuven, Belgium, in 2008.

Currently, he is the R&D Team Leader at imec, Leuven, Belgium, where he is leading the activities on analog integrated circuit design for portable and implantable biomedical applications. During his research, he has coauthored more than 70 publications, three book chapters, and a book on ultra-low-power circuit and system design for biomedical applications. He has developed several generations of integrated circuits for wearable and implantable healthcare applications.

Dr. Yazicioglu was the co-recipient of the Best Student Paper Award at the IEEE International Symposium on Circuits and Systems (ISCAS) 2013, IEEE Biomedical Circuits and System Conference (BioCAS) 2011, Smart Systems Integration (SSI) Conference, 2008, and Sensors and Transducers Journal 2008. He serves on the technical program committees of European Solid State Circuits (ESSCIRC) and International Solid State Circuit Conference (ISSCC). He was cochair of the Biomedical Circuits and Systems Conference (BioCAS) 2013 in Rotterdam, The Netherlands.

Trac D. Tran (S'94–M'98–SM'08) received the B.S. and M.S. degrees from the Massachusetts Institute of Technology, Cambridge, MA, USA, in 1993 and 1994, respectively, and the Ph.D. degree from the University of Wisconsin, Madison, WI, USA, in 1998, all in electrical engineering.

In July 1998, he joined the Department of Electrical and Computer Engineering, The Johns Hopkins University, Baltimore, MD, USA, where he currently holds the rank of Associate Professor. In the summer of 2002, he was an ASEE/ONR Summer Faculty Research Fellow at the Naval Air Warfare Center Weapons Division at China Lake, CA, USA. He is a regular Consultant for the U.S. Army Research Laboratory, Adelphi, MD, USA. His research interests are in the field of digital signal processing, particularly in sparse representation, sparse recovery, sampling, multirate systems, filter banks, transforms, wavelets, and their applications in signal analysis, compression, processing, and communications. His pioneering research on integer-coefficient transforms and pre-/post-filtering operators has been adopted as critical components of Microsoft Windows Media Video 9 and JPEG XRthe latest international still-image compression standard ISO/IEC 29199-2.

Dr. Tran was the Codirector (with Prof. J. L. Prince) of the 33rd Annual Conference on Information Sciences and Systems (CISS 99), Baltimore, MD, in March 1999. He has served as an Associate Editor of the IEEE TRANSACTIONS ON SIGNAL PROCESSING as well as IEEE TRANSACTIONS ON IMAGE PROCESSING. He was a former Member of the IEEE Technical Committee on Signal Processing Theory and Methods (SPTM TC) and is a current member of the IEEE Image Video and Multidimensional Signal Processing Technical Committee. He received the NSF CAREER Award in 2001, the William H. Huggins Excellence in Teaching Award from The Johns Hopkins University in 2007, and the Capers and Marion McDonald Award for Excellence in Mentoring and Advising in 2009.

Ralph Etienne-Cummings (F'13) received the B.Sc. degree in physics from Lincoln University, Lincoln, PA, USA, in 1988, and the M.S.E.E. and Ph.D. degrees in electrical engineering from the University of Pennsylvania, Philadelphia, PA, USA, in 1991 and 1994, respectively.

Currently, he is a Professor of electrical and computer engineering, and computer science with The Johns Hopkins University (JHU), Baltimore, MD, USA. He is the former Director of computer engineering at JHU and the Institute of Neuromorphic Engineering. He is also the Associate Director for Education and Outreach of the National Science Foundation (NSF) sponsored Engineering Research Centers on Computer Integrated Surgical Systems and Technology at JHU. His current research interests include mixed signal VLSI systems, computational sensors, computer vision, neuromorphic engineering, smart structures, mobile robotics, legged locomotion and neuroprosthetic devices.

Dr. Etienne-Cummings has served as the Chairman of the IEEE Circuits and Systems (CAS) Technical Committee on Sensory Systems and on Neural Systems and Application. He was also the General Chair of the IEEE BioCAS 2008 Conference. He was a member of Imagers, MEMS, Medical and Displays Technical Committee of the ISSCC Conference from 1999 to 2006. He is a recipient of the NSFs Career and Office of Naval Research Young Investigator Program Awards. In 2006, he was named a Visiting African Fellow and a Fulbright Fellowship Grantee for his sabbatical with the University of Cape Town, Cape Town, South Africa. He was invited to be a Lecturer with the National Academies of Science Kavli Frontiers Program, in 2007. He was a recipient of publication awards including the 2003 Best Paper Award of the *EURASIP Journal of Applied Signal Processing* and the Best Ph.D. in a Nutshell at the IEEE BioCAS 2008 Conference. He has been recognized for his activities in promoting the participation of women and minorities in science, technology, engineering and mathematics.